

Multilayer metamaterial absorbers inspired by perfectly matched layers

Anna Pastuszcak · Marcin Stolarek ·
Tomasz J. Antosiewicz · Rafał Kotyński

Received: date / Accepted: date

Abstract We derive periodic multilayer absorbers with effective uniaxial properties similar to perfectly matched layers (PML). This approximate representation of PML is based on the effective medium theory and we call it an effective medium PML (EM-PML). We compare the spatial reflection spectrum of the layered absorbers to that of a PML material and demonstrate that after neglecting gain and magnetic properties, the absorber remains functional. This opens a route to create electromagnetic absorbers for real and not only numerical applications and as an example we introduce a layered absorber for the wavelength of $8\text{ }\mu\text{m}$ made of SiO_2 and NaCl . We also show that similar cylindrical core-shell nanostructures derived from flat multilayers also exhibit very good absorptive and reflective properties despite the different geometry.

Keywords electromagnetic absorber · metamaterial · electromagnetic modeling · perfectly matched layer · UPML

1 Introduction

Perfectly matched layer (PML) (Berenger, 2007) absorbers are now widely used to terminate electromagnetic simulations with an open domain. PMLs suppress reflection and ensure absorption of incident electromagnetic radiation at any angle and any polarization. A variety of PML formulations exist, starting from the early split-field PML (Berenger, 1994), and the coordinate stretching approach (Chew and Weedon, 1994) up to the convolutional PML (CPML) (Roden and Gedney, 2000), and the near

This work was supported by research project UMO-2011/01/B/ST3/02281 of the Polish National Science Center. PL-Grid infrastructure is acknowledged for providing access to computational resources.

A. Pastuszcak · M. Stolarek · R. Kotyński ✉
Faculty of Physics, University of Warsaw, Pasteura 7, 02-093 Warsaw, Poland
E-mail: rafalk@fuw.edu.pl, Tel.: +48-225546888, Fax: +48-225546882

T. J. Antosiewicz
Centre of New Technologies, University of Warsaw, Żwirki i Wigury 93, 02-089 Warsaw, Poland
Department of Applied Physics and Gothenburg Physics Centre, Chalmers University of Technology, SE-41296 Göteborg, Sweden

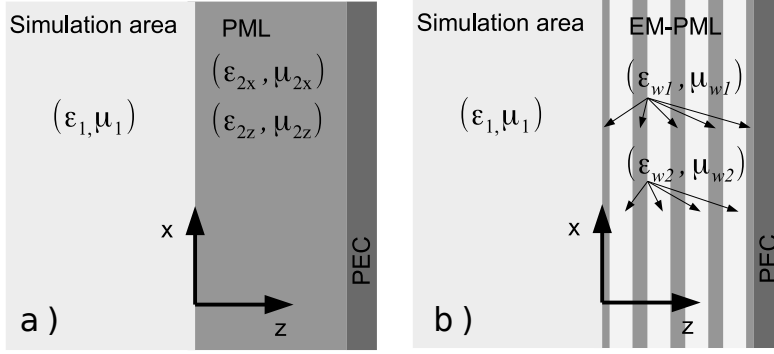


Fig. 1 a) A uniaxial PML characterized by anisotropic permittivity and permeability tensors is attached to a simulation area (ϵ_1, μ_1) . b) An effective-medium PML, which has the same uniaxial properties, can be composed of two isotropic materials $(\epsilon_{wi}, \mu_{wi})$, where $i = 1, 2$ arranged in a multilayered fashion. In both cases a perfect electric conductor (PEC) terminates the PML

PML (NPML)(Cummer, 2003). In this paper we refer to the Maxwellian formulation of PML, represented by an artificial material with uniaxial permittivity and permeability tensors, usually termed as uniaxial PML (UPML) (Sacks et al, 1995; Gedney, 1996). A PML can be used with both time-domain and frequency domain methods, as well as with finite difference or finite element discretization schemes. It can assume various dispersion models, see e.g. the time-derivative Lorentz material that is capable of absorbing oblique, pulsed electromagnetic radiation having narrow and broad waists (Ziolkowski, 1997). A PML can not be applied in some rare cases and for instance it fails to absorb a backward propagating wave for which an adiabatic absorber should be used instead (Zhang et al, 2008; Loh et al, 2009).

Electromagnetic absorbers have a much longer history than any kind of numerical modeling. Their possible applications range from modification of radar echo, through applications related to electromagnetic compatibility, up to photovoltaics. Early real-world absorbers were based on resistive sheets separated from a ground plate by quarter wave distances. With several sheets and multiple resonances it was possible to achieve broadband operation. The idea evolved into the theory of frequency selective surfaces (Munk, 2000). Furthermore, it is possible to obtain a tailored impedance at a surface transition region using homogenized periodic one-dimensional or two-dimensional corrugated surfaces (Kristensson, 2005). A static periodic magnetization obtained with ferromagnetic or ferrimagnetic materials is another route to obtaining broadband absorbers (Ramprecht and Norgren, 2008). A recent overview paper (Watts et al, 2012) can serve as a tutorial on absorbers with the focus on novel metamaterial absorbers based on split-ring and electric-ring resonators.

In this paper we introduce the effective medium PML absorbers (EM-PML), which are metamaterial absorbers with a layered structure that exhibit effective permittivity and permeability tensors similar to a PML material. We calculate the reflection coefficient achieved with these layered absorbers. We look towards their possible physical realizations.

2 Approximate representation of UPML

A schematic of a uniaxial perfectly matched layer attached to a simulation area is shown in Fig. 1. In the outer area of the simulation domain (which neighbors the PML), the permittivity and permeability are equal to ε_1 , and μ_1 . The UPML is defined as a material whose permittivity ε_2 and permeability μ_2 take the following tensor forms,

$$\varepsilon_2 = \begin{bmatrix} \varepsilon_{2x} & 0 & 0 \\ 0 & \varepsilon_{2x} & 0 \\ 0 & 0 & \varepsilon_{2z} \end{bmatrix}, \quad \mu_2 = \begin{bmatrix} \mu_{2x} & 0 & 0 \\ 0 & \mu_{2x} & 0 \\ 0 & 0 & \mu_{2z} \end{bmatrix}, \quad (1)$$

where

$$\varepsilon_{2x} = s \cdot \varepsilon_1, \quad \mu_{2x} = s \cdot \mu_1, \quad \varepsilon_{2z} = s^{-1} \cdot \varepsilon_1, \quad (2)$$

and

$$\mu_{2x} = s \cdot \mu_1, \quad \varepsilon_{2x} = s \cdot \varepsilon_1, \quad \mu_{2z} = s^{-1} \cdot \mu_1. \quad (3)$$

The parameter s is a non-zero freely chosen complex number, whose imaginary part determines the strength of absorption within the UPML. The conditions stated in Eq. (2) alone are sufficient to remove reflections for the TM polarization, for any plane-wave propagating in-plane, independently of its angle of incidence and frequency. Equation (3) assures the same for the TE polarization and when both conditions are satisfied, the UPML is reflection-free for any polarization and any angle of incidence in a three-dimensional case. Subsequently, s may be varied with the coordinate z to give a continuously graded permittivity and permeability, which works better with most discretization schemes. Then, the same parameter s may also be linked to a coordinate mapping from real to complex coordinates.

Our approximate representation of a UPML consists of a one-dimensional stack of uniform layers. According to the effective medium theory (EMT) a stack consisting of thin layers may be homogenized and replaced by a uniform uniaxial medium with effective permittivity and permeability tensors. For the TM polarization, the effective permittivity and permeability tensors of a stack consisting of two materials with permittivity and permeability pairs $(\varepsilon_{w1}, \mu_{w1})$, and $(\varepsilon_{w2}, \mu_{w2})$ match that of a UPML, expressed by Eq. (1), when

$$f \cdot \varepsilon_{w1} + (1 - f) \cdot \varepsilon_{w2} = s \cdot \varepsilon_1, \quad (4)$$

$$[f \cdot \varepsilon_{w1}^{-1} + (1 - f) \cdot \varepsilon_{w2}^{-1}]^{-1} = s^{-1} \cdot \varepsilon_1, \quad (5)$$

$$f \cdot \mu_{w1} + (1 - f) \cdot \mu_{w2} = s \cdot \mu_1, \quad (6)$$

where f is the filling factor, i.e. the volume fraction of material $w1$ in the stack. A similar condition applies for the TE polarization. Solving equations (4) and (5) for ε_{w1} , and ε_{w2} yields,

$$\varepsilon_{w1} = \rho \cdot \frac{\varepsilon_1 \cdot s}{f \cdot \rho + (1 - f)}, \quad \varepsilon_{w2} = \frac{\varepsilon_1 \cdot s}{f \cdot \rho + (1 - f)}, \quad (7)$$

where

$$\rho = 1 + \frac{s^2 - 1 \pm \sqrt{(s^2 - 1)(s^2 - (2f - 1)^2)}}{2f(1 - f)}. \quad (8)$$

In Fig. 2 we illustrate the permittivities calculated from eq. (7) as a function of the fill factor f and s , for $s = 1 + \alpha i$. We use the branch of Eq. (8) with $|\rho| > 1$.

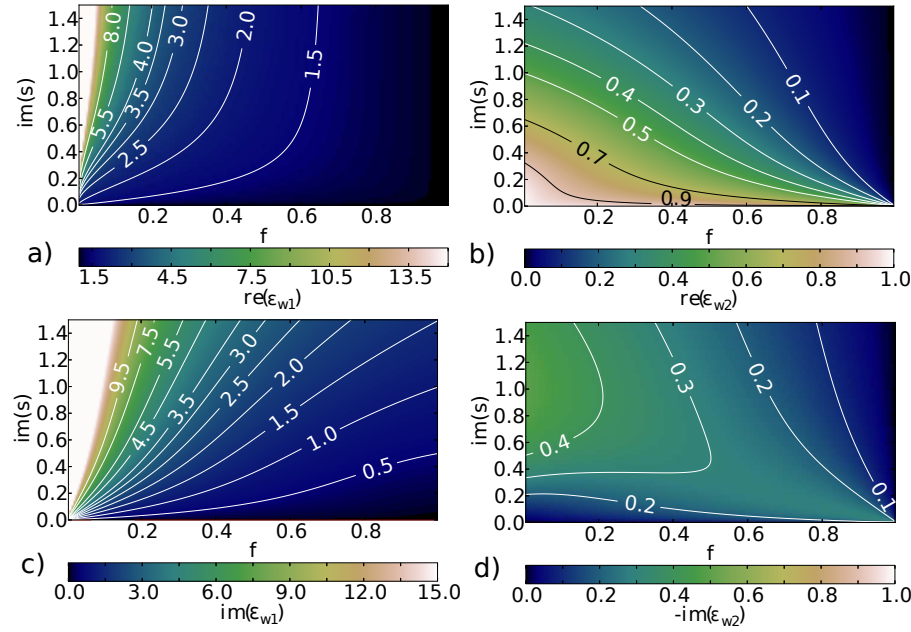


Fig. 2 Permittivities of the two constituent isotropic media (ε_{w1} and ε_{w2} in left and right columns, respectively) that form the uniaxial EM-PML as functions of the filling factor f and the imaginary part of s (for $\text{re}(s) = 1$). Top row: real parts (a) $\text{re}(\varepsilon_{w1})$ and (b) $\text{re}(\varepsilon_{w2})$. Bottom row: imaginary parts (c) $\text{im}(\varepsilon_{w1})$ and (d) $-\text{im}(\varepsilon_{w2})$. Negative imaginary part of permittivity refers to materials with optical gain. Qualitatively, one of the materials is a high-loss material with a large refractive index (greater than one), while the other is a low-gain medium with a refractive index between 0 and 1

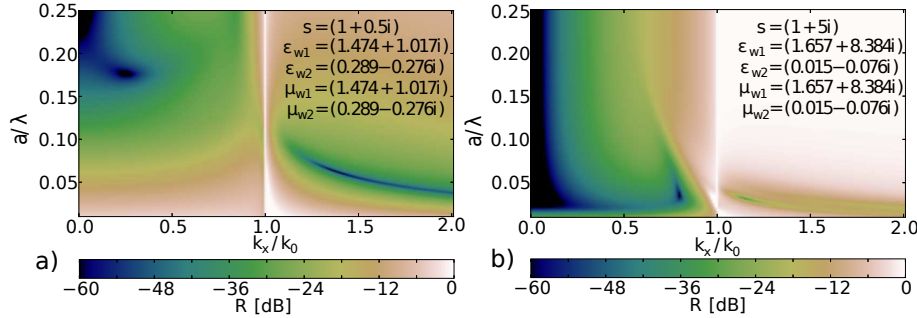


Fig. 3 Dependence of spatial reflection spectrum $R(k_x/k_0)$ on a/λ for a multilayer consisting of $N = 5$ periods obtained with $f = 0.6$ and a) $s = 1 + 0.5i$, b) $s = 1 + 5i$. The result is polarization invariant

Expressions similar to Eqs. (4) and (5) may be written and solved for μ_{w1} , and μ_{w2} , and when $\varepsilon_1 = \mu_1$ then $\varepsilon_{w1} = \mu_{w1}$ and $\varepsilon_{w2} = \mu_{w2}$.

An absorber designed for the TM polarization may have one of the permeabilities freely assigned, e.g. $\mu_{w2} = 1$, while the other is then given by Eq. (6). If additionally $s = 1 + \alpha i$ then $\text{re}(\mu_{w2}) = 1$ and the imaginary part of μ_{w2} for this case is still positive, as shown in Fig. 4. The imaginary part of μ_{w2} is small when f is large and α is small.

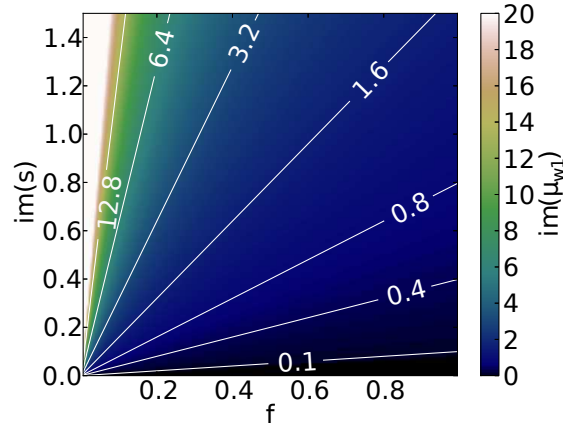


Fig. 4 Imaginary part of permeability of one of the materials of the EM-PML μ_{w1} as a function of the filling factor f and the imaginary part of s (for $\text{re}(s) = 1$). Here, we have assumed that the permeability of the second material is unity $\mu_{w2} = 1$, as can be done for TM polarized light, and $\text{re}(\mu_{w1}) = 1$

For either large f or small α the negative conductivity of the second material is also negligible (see Fig. 2d).

The performance of a multilayer absorber obtained for $f = 0.6$ and $s = 1 + 0.5i$, and $s = 1 + 5i$ is illustrated in Fig. 3. Either of the two values of s enables to construct an efficient broadband absorber which is at the same time subwavelength in size. Layers have both magnetic and electric properties, including gain, and a complex permeability. In the limit of $a/\lambda \rightarrow 0$ the multilayer approaches the properties of a true UPML (but at the same time, its thickness approaches $N \cdot a \rightarrow 0$). When $s = 1 + 5i$, an absorber consisting of $N = 5$ periods, with a total thickness of $L = 5a \approx \lambda/20$ reflects -30dB for a broad range of incidence angles, and the reflection decreases rapidly with total thickness L/λ . However, the evanescent waves are amplified in this situation. If the absorbing power is smaller, e.g. $s = 1 + 0.5i$, the thickness L/λ has to be larger, but the reflection is less sensitive to the magnetic permeability and gain.

Let us assess how the reflection spectrum is changed after the magnetic permeabilities and gain have been neglected. The result is depicted in Fig. 5 for $s = 1 + 0.5i$ and $f = 0.6$. The absorber consists of layers made of a lossy dielectric and of another material with permittivity lower than one. A probable route to implement it physically is to use a metamaterial, e.g. a fishnet structure, to make use of electromagnetic mixing rules, or to use some material near its resonance frequency. Now the reflection coefficient depends on polarization. Before neglecting gain and $\text{im}(\mu_{w1})$, the reflection has been smaller for the TM than for the TE polarization, both for the propagating and for evanescent waves. Reflection remained large only at grazing incident angles, like for ordinary UPML. However, the variant of the stack with no gain and with no magnetic properties performs better for the TE polarization (See Fig. 5bd).

Finally, the multilayer considered here has an elliptical effective dispersion relation, while similar absorbers made of hyperbolic metamaterials have been also recently proposed (Guclu et al, 2012), although with no relation to PML.

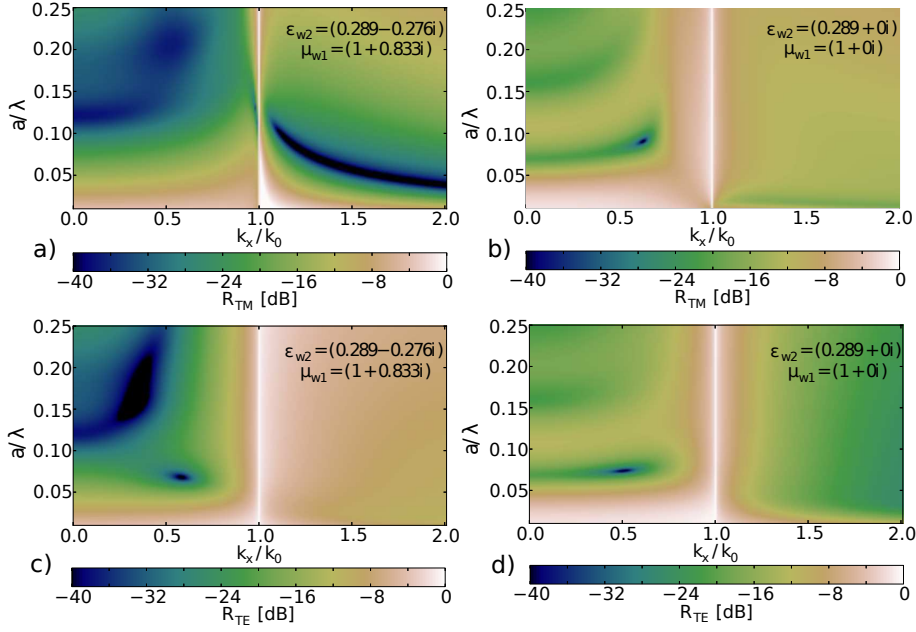


Fig. 5 Dependence of spatial reflection spectrum $R(k_x/k_0)$ on a/λ for a multilayer consisting of $N = 5$ periods obtained for $f = 0.6$, $s = 1 + 0.5i$ with the assumption that $\mu_{w2} = 1$ (a,c), and with the assumptions that $\mu_{w1} = \mu_{w2} = 1$ and $\text{im}(\epsilon_{w1}) \geq 0$, $\text{im}(\epsilon_{w2}) \geq 0$ (b,d). Reflection is calculated for the TM (a,b) and TE (c,d) polarizations. The permittivity ϵ_{w1} equals $1.474 + 1.017i$

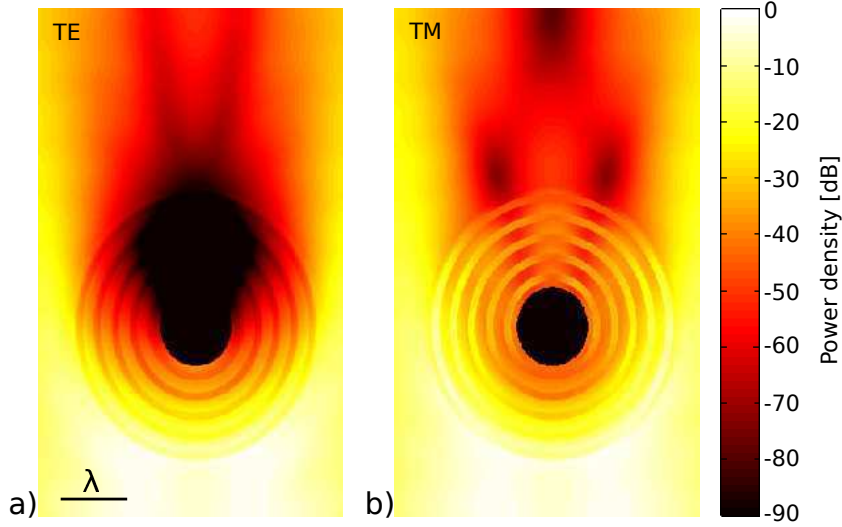


Fig. 6 FDTD simulation of the operation of a nonmagnetic layered absorber deposited on a cylindrical metallic object for the a) TE-polarization, and b) TM-polarization. The scalebar of 1λ is included in the figure. The composition of the absorber is the same as in Figs. 5cd, with $a/\lambda = 0.18$

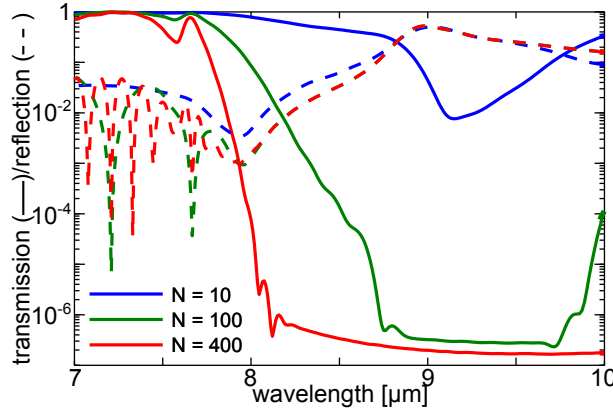


Fig. 7 Transmission (continuous line) and reflection (dashed) for a SiO_2/NaCl multilayer designed to absorb at $8 \mu\text{m}$ at which the refractive indices are $n_{\text{SiO}_2} = 0.41 + 0.32i$, $n_{\text{NaCl}} = 1.51$, SiO_2 , fill factor $f = 0.56$, $a = 200 \text{ nm}$. The number of periods is $N = 10, 100, 400$

3 Layered slab and core-shell metamaterial absorbers

Based on the theoretical considerations and material parameters used to calculate the spatial reflection spectrum in Fig. 5, a simple rule of thumb for the range of required permittivities can be drawn up. This simple rule requires one permittivity to have its real part between 0 and 1, while the other permittivity would have its real part larger than one. The calculations show, that losses should be provided by the second material (with $\text{Re}(\epsilon) > 1$), while in the first material we merely neglect gain. Materials in general have $\text{Re}(\epsilon) > 1$, with the exception of localized transitions and broader frequency ranges in metals up to the plasma frequency.

We will now demonstrate the operation of the proposed layered absorber consisting of nonmagnetic layers with no gain. In Fig. 6 we present the results of a finite difference time domain (FDTD) simulation of a layered absorber rolled into a cylindrical core-shell multilayer. The images show the time-averaged energy density distribution obtained for the TE polarization (in Fig. 6a) and TM polarization (in Fig. 6b). Light is incident from the bottom side. The composition of the metamaterial is the same as in Figs. 5cd, but the multilayer is deposited over a cylindrical metallic (perfectly conducting) material. The absorber consists of $N = 5$ periods of non-magnetic concentric layers, with the radial pitch equal to $a = 0.18\lambda$, the radius of the internal PEC material is equal to $r_{\text{int}} = 2a$, and the external radius is equal to $r_{\text{ext}} = 7a$. The permittivities of the layers are equal to $\epsilon_{w1} = 1.474 + 0.017i$, and $\epsilon_{w2} = 0.289$, and the filling factor equals $f = 0.6$. Reflections, understood as the part of the energy backscattered to the bottom side of the simulation area are as small as $R_{TE} = 0.05\%$, and $R_{TM} = 0.3\%$. Thanks to the cylindrical geometry, it is possible to see the operation of the absorber at all possible angles of incidence at the same time. Notably the absorber performs well both for the TE and TM polarization, and in a spherical 3D core-shell geometry where there is no decoupling into these two polarizations we expect similar operation.

Finally, we demonstrate the operation of a layered absorber consisting of real materials. Here, we make use of materials with localized electronic transitions. In the mid-infrared SiO_2 is such a material, which features a strong transition at approximately $9 \mu\text{m}$ and in a range between 7.2 and $8 \mu\text{m}$ its real part of permittivity is

between 1 and 0. The complementary material of choice is NaCl, which in this range has $\text{Re}(\epsilon) \approx 1.5$, however, it also is weakly dispersive in this range and due to Kramers-Kronig relations between the real and imaginary parts of permittivity it has a very small imaginary part. Thus, SiO₂ needs to provide dissipation to extinguish the incident beam. Deposition of alternating SiO₂ and NaCl or LiF layers of required thickness may be accomplished using such techniques as chemical vapor deposition or thermal evaporation (Fornarini et al, 1999; Kim and King, 2007), although with the required total thickness of the layers approaching a few wavelengths, a fast method is preferable, at least for absorbers intended for infrared.

Fabrication of multilayered shell structures is more challenging, although synthesis of core/shell nanoparticles incorporating SiO₂ or Al₂O₃ and noble metals is commonplace nowadays (Liu et al, 2014; Wang et al, 2014; Mai et al, 2011). In the considered case here, it would be required to synthesize a layered spherical particle consisting of only dielectric materials. As mentioned previously, SiO₂ and Al₂O₃ have been used before, although only in relatively simple synthesis of core-shell structures; magnesium fluoride has also been synthesised in the form of nanoparticles (Lellouche et al, 2012). However, undoubtedly some effort would be required to develop a procedure for the synthesis of layered nanoparticles. In Fig. 7 we present the results obtained for a plane wave incident normally onto a SiO₂/NaCl multilayer designed for the 7-10 μm wavelength range. The refractive index of the materials is taken from literature (Palik, 1985) and the structure is optimized for $\lambda = 8 \mu\text{m}$. The pitch is equal to $a = 200 \text{ nm}$, and the filling factor is $f = 0.56$. Due to small losses in glass, the absorption distance is relatively long and reflection smaller than 1% is observed already for 10 layers. In order to achieve both transmission and reflection smaller than 0.1% $N = 400$ is needed. The thickness can be reduced using materials with larger values of the imaginary part of permittivity.

In general, a desired refractive index of one of the layers (in the range $0 < \Re(n) < 1$) can be manufactured using the electromagnetic mixing rules. Recently, absorbers made of hyperbolic metamaterials have been proposed (Guclu et al, 2012) and similar to that material, our multilayer has an elliptical dispersion with a large eccentricity.

4 Conclusions

We have introduced an approximate representation of the uniaxial perfectly matched layer reflection-free absorber. The representation consists of a one-dimensional stack of uniform and isotropic metamaterial layers. A further simplification to non-magnetic materials with no gain can be assumed for some combinations of filling fraction and absorbing power. We have also shown that similar cylindrical core-shell nanostructures derived from flat multilayers also exhibit very good absorptive and reflective properties. A probable route to implement the absorber experimentally is by using a lossy dielectric as one material and for the other to take a metamaterial, or to make use of electromagnetic mixing rules, or to use some material near its resonance frequency. As an example we have demonstrated a layered absorber for the wavelength of 8 μm made of SiO₂ and NaCl.

References

- Berenger J A perfectly matched layer for the absorption of electromagnetic waves. *J Computational Physics* 114:185–200, 1994
- Berenger JP (2007) Perfectly Matched Layer (PML) for Computational Electromagnetics. Morgan and Claypool Publishers
- Chew WC, Weedon WH A 3D perfectly matched medium from modified Maxwell's equations with stretched coordinates. *IEEE Microwave and Guided Wave Letters* 7:599–604, 1994
- Cummer SA A simple, nearly perfectly matched layer for general electromagnetic media. *IEEE Wirel Lett* 13:128–130, 2003
- Fornarini L, Mancini A, Martelli S, Montereal R, Picozzi P, Santucci S Structural properties and photoluminescence spectra of coloured LiF films on SiO₂. *Journal of Non-Crystalline Solids* 245:141–145, 1999
- Gedney SD An anisotropic perfectly matched layer-absorbing medium for the truncation of FDTD lattices. *IEEE Trans Antennas Propagat* 44:1630–1639, 1996
- Guclu C, Campione S, Capolino F Hyperbolic metamaterial as super absorber for scattered fields generated at its surface. *Phys Rev B* 86:205,130, 2012
- Kim H, King AH Control of porosity in fluoride thin films prepared by vappor deposition. *J Mater Res* 22:2012–2016, 2007
- Kristensson G Homogenization of corrugated interfaces in electromagnetics. *PIER* 55:1–31, 2005
- Lellouche J, Friedman A, Lellouche JP, Gedanken A, Banin E Improved antibacterial and antibiofilm activity of magnesium fluoride nanoparticles obtained by water-based ultrasound chemistry. *Nanomedicine: Nanotechnology, Biology and Medicine* 8:702–711, 2012
- Liu J, Kan C, Cong B, Xu H, Ni Y, Li Y, Shi D Plasmonic property and stability of core-shell AuSiO₂ nanostructures. *Plasmonics* 10.1007/s11468-014-9708-1, 2014
- Loh PR, Oskoo AF, Ibanescu M, Skorobogatiy M, Johnson SG Fundamental relation between phase and group velocity, and application to the failure of perfectly matched layers in backward-wave structures. *Phys Rev E* 79, 065601R, 2009
- Mai FD, Yu CC, Liu YC, Yang KH, Juang MY Preparation of surface-enhanced Raman scattering-active Au/Al₂O₃ colloids by sonoelectrochemical methods. *J Phys Chem C* 115:13,660–13,666, 2011
- Munk BA (2000) Frequency Selective Surfaces. John Wiley & Sons, New York
- Palik ED (ed) (1985) Handbook of Optical Constants of Solids, vol 1. Academic Press: New York
- Ramprecht J, Norgren M Scattering from a thin magnetic layer with a periodic lateral magnetization: application to electromagnetic absorbers. *PIER* 83:199–224, 2008
- Roden JA, Gedney SD Convolutional PML (CPML): An efficient FDTD implementation of the CFE-PML for arbitrary media. *Microw Opt Technol Lett* 27:334–339, 2000
- Sacks ZS, Kingsland DM, Lee R, Lee JF A perfectly matched anisotropic absorber for use as an absorbing boundary condition. *IEEE Trans Antennas Propagat* 43:1460–1463, 1995
- Wang HS, Wang C, He YK, Xiao FN, Bao WJ, Xia XH, Zhou GJ Core-shell Ag-SiO₂ nanoparticles concentrated on a micro/nanofluidic device for surface plasmon resonance-enhanced fluorescence detection of highly reactive oxygen species. *Anal Chem* 86:3013–3019, 2014

-
- Watts CM, Liu X, Padilla WJ Metamaterial Electromagnetic Wave Absorbers. *Adv Mater* 24:OP98–OP120, 2012
- Zhang L, Avniel Y, Johnson SG The failure of perfectly matched layers, and towards their redemption by adiabatic absorber. *Opt Express* 16:11,376–11,392, 2008
- Ziolkowski RW The design of maxwellian absorbers for numerical boundary conditions and for practical applications using engineered artificial materials. *IEEE Trans Antennas Propagat* 45:656–671, 1997